PHYSICAL REVIEW B VOLUME 61, NUMBER 10 1 MARCH 2000-II

Finite-size effects in nickel nanowire arrays

L. Sun and P. C. Searson
Department of Materials Science and Engineering, The Johns Hopkins University, Baltimore, Maryland 21218

C. L. Chien
Department of Physics and Astronomy, The Johns Hopkins University, Baltimore, Maryland 21218

(Received 11 June 1999)

Nickel nanowire arrays with diameters in the range 30–500 nm have been fabricated by electrochemical deposition into nanoporous, single-crystal mica templates, which allow measurements of the magnetic properties of nickel nanowire arrays at high temperatures. The Curie temperature is found to be reduced by as much as 51 K for the 30 nm diameter nanowires. The Curie temperature shift with wire diameter follows the finite-size scaling relation with $\lambda = 0.94$ and $\xi_0 = 22$ Å.

The influence of reduced physical dimensions on magnetic entities is of both fundamental and technological interest. In bulk magnetic systems, the correlation length ξ increases with temperature and diverges at the bulk transition temperature $T_C(\infty)$. When one or more dimensions in the system are small, the growth of ξ will eventually be limited by the smallest dimension d and the system displays a reduced transition temperature $T_C(d)$ due to finite-size effects. Technologically, as the feature sizes of magnetic structures continue to decrease, the influence of dimensionality on their magnetic properties has also become an important issue. To date, reports of finite-size effect in magnetic systems have been largely limited to ultrathin films and quasi-two-dimensional systems. Measurements on quasi-one-dimensional systems have been hampered by the difficulty in fabricating structures that are sufficiently small and stable over the required temperature range.

In quasi-two-dimensional systems, thickness dependent phase transition temperatures have been measured in ultrathin ferromagnetic films of Ni,[1–6] Fe,[7,8] Co,[9] and Gd (Refs. 10–12) and CuMn spin glass films.[13,14] Recently, finite-size effects have also been reported in antiferromagnetic CoO (Refs. 15 and 16) and Cr (Ref. 17) thin films. In quasizero dimensional systems, such as granular thin films, phase transitions are not observed due to the onset of superparamagnetism when the particle size is very small.[18]

Electrochemical deposition of metals into porous polymer films has been used to fabricate quasi-one-dimensional nanowire arrays[19–22] and the ferromagnetic properties of Ni and Co have been studied both at low temperatures and at room temperature.[22–25] However, measurements of magnetic phase transitions are not possible in these structures since the Curie temperatures for elements such as Ni, Co, and Fe are much higher than the temperature range of polymer templates. In this paper we describe the fabrication of quasi-one-dimensional nickel nanowire arrays in porous mica films and show that this approach can be used to determine the temperature dependence of the magnetic properties at elevated temperatures.

Nickel nanowire arrays were fabricated by electrochemical deposition into porous single-crystal muscovite mica templates. Mica is chemically stable up to 770 K, well above the Curie temperature for bulk Ni (~630 K). The porous templates were fabricated by nuclear track etching. Particle tracks were formed in 5 μm thick mica wafers by exposure to ≈6 meV α particles from a 100 μCiCf-252 source in a chamber at a pressure of about 10^{-3} Torr. The alignment of the particle tracks was within 5° through collimation of the α-particle beam. The particle tracks were etched by immersing the tracked wafers in 20 wt. % HF at room temperature. From electrical conductance measurements we determined the etch rate of the particle tracks to be about 1200 Å s^{-1}.[26] The lateral etch rate of the bulk mica was determined to be 0.35 Å s^{-1}.[26] From the ratio of the normal and lateral etch rates we determine that the taper on the pore walls due to etching is 0.02°. Pore diameters in the range 30–500 nm were obtained by varying the etching time. In order to minimize the number of overlapping pores, the volume fraction of nickel in the films was set at about 0.02 for all samples by adjusting the track density from 1×10^7 cm^{-2} for the 500 nm pores to 2×10^9 cm^{-2} for the 30 nm diameter pores. The relevant parameters are shown in Table I. For a volume fraction of 0.02, the fraction of tracks resulting in overlapping pores is less than 4%.[26]

Figure 1 shows a scanning electron microscope image of etched particle tracks in mica. The pores are perpendicular to the film plane and the pore walls are smooth and free from etching residues. The pores are diamond shaped with the pore walls defined by the {110} planes corresponding to the oxygen terminated planes in the mica lattice.[25] For convenience the pore diameter is defined as the diameter of the

TABLE I. Effective diameter (d), number density of tracks (n), and volume (area) fraction (f) of pores.

d (nm)	n (cm^{-2})	f
500	1×10^7	0.0196
200	5×10^7	0.0157
150	1×10^8	0.0177
100	3×10^8	0.0236
50	1×10^9	0.0196
30	2×10^9	0.0141

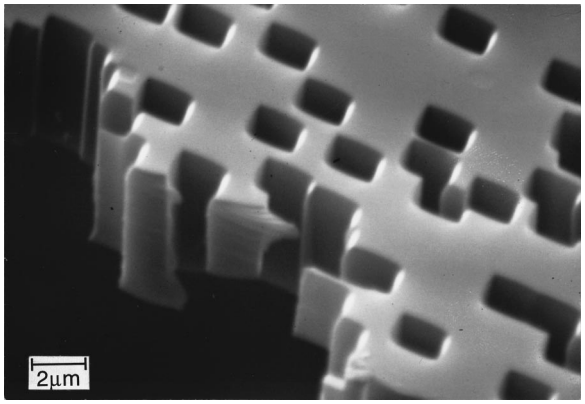

FIG. 1. Scanning electron microscope image of 2 μm pores in single-crystal mica.

circle having the same cross-sectional area as the diamond-shaped pores.

Nickel nanowire arrays were fabricated by electrochemical deposition into the mica templates. The electrode contact was provided by a sputter deposited gold layer. Nickel was deposited from a solution of 20 $g\,l^{-1}$ $NiCl_2 \cdot 6H_2O$, 515 $g\,l^{-1}$ $Ni(H_2NSO_3)_2 \cdot 4H_2O$, 20 $g\,l^{-1}$ H_3BO_3 buffered to pH 3.4 at a potential of -1.0 V (Ag/AgCl).[25] Scanning electron microscopy and atomic force microscopy were used to verify that ~100% of the pores were filled during the deposition process and that the nickel nanowires grew at a similar rate. An advantage of this geometry is that the nickel nanowires are embedded in the mica films, reducing oxidation and structural damage at elevated temperatures.[27]

After dissolving the mica matrix in concentrated HF(~48 wt. %), free standing Ni nanowires were obtained on the gold electrode. Figure 2 shows an SEM image of free standing 150 nm nanowires. In the cross section the wires have a diamond shape due to conformal filling of the diamond shaped pores in the mica.

The magnetization measurements were conducted on a vibrating sample magnetometer. Due to the strong shape anisotropy of the nickel nanowires, the applied external magnetic field was parallel to the wire axis. The room-temperature magnetic coercivity of the nickel nanowire arrays increases with decreasing wire diameter, reaching values of 800–900 Oe for 30 nm diameter wires.[22–25] The

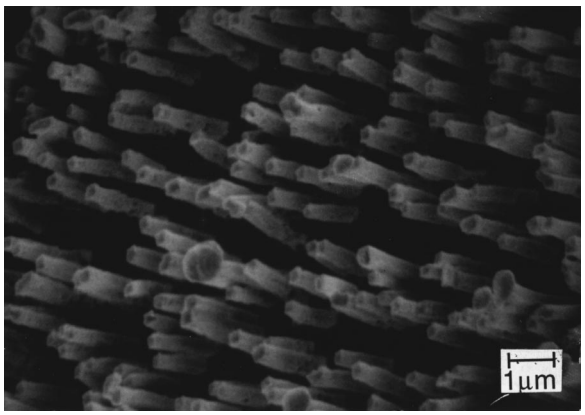

FIG. 2. Scanning electron microscope image of 150 nm diameter Ni nanowires after etching of the mica template.

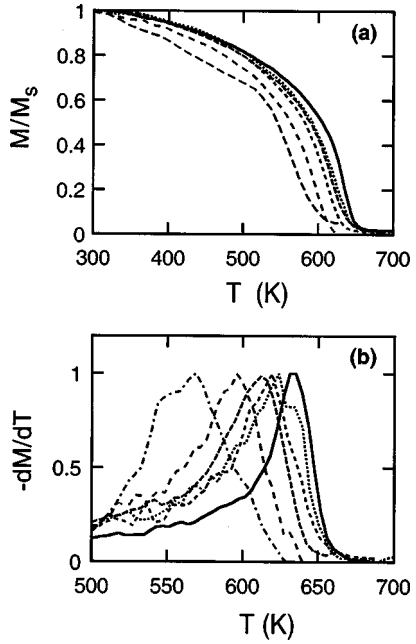

FIG. 3. (a) Normalized magnetization and (b) normalized derivatives of the *M-T* curves vs temperature for nickel nanowire arrays with diameters (from left to right) of 30, 50, 100, 150, 200, and 500 nm. The solid curves correspond to bulk nickel. All measurements were obtained at $H = 2000$ Oe.

squareness (the ratio of the remanence and saturation magnetization) is strongly dependent on the physical properties of the porous template, particularly the alignment of the pores. Recently, we have shown[25] that values of the squareness as high as 0.96 can be obtained with mica templates due to the improved collimation of the pores, the uniform pore cross section, and the low density of overlapping pores.

Figure 3(a) shows *M-T* curves for nickel nanowire arrays as a function of the wire diameter from 30 to 500 nm. The temperature was calibrated prior to each measurement using a bulk nickel sample. Figure 3(b) shows the derivative of the *M-T* curves from which we determined the Curie temperature; identical results were obtained from examination of the hysteresis loops. These results clearly show that the Curie temperature progressively decreases with decreasing wire diameter. The Curie temperatures obtained by this method were independent of the applied magnetic field over the measured range 2 000 to 12 000 Oe. Figure 4(a) shows the dependence of the measured Curie temperature on the wire diameter.

The reduction of the Curie temperature for nanowires with decreasing diameter is due to finite-size effects. The correlation length $\xi(T)$ of a magnetic system increases with temperature and at temperatures close to the bulk transition temperature $T_C(\infty)$, the correlation length $\xi(T)$ has an asymptotic behavior described by

$$\xi(T) = \xi_0 \left| 1 - \frac{T}{T_C(\infty)} \right|^{-\nu}, \tag{1}$$

where ξ_0 is the correlation length extrapolated to $T = 0$, and ν is the critical exponent for correlation.[28] For a magnetic system with a small dimension of size d (e.g., the diameter of the nanowires), the growth of $\xi(T)$ with increasing tempera-

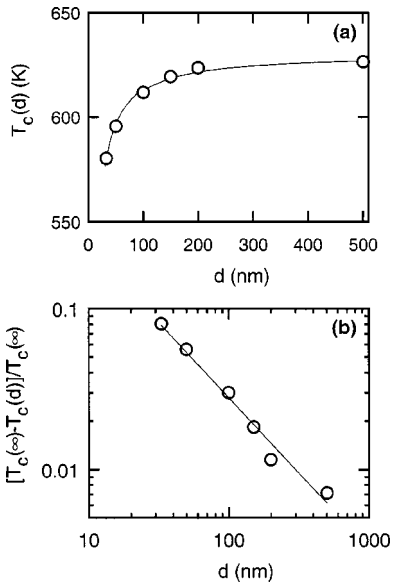

FIG. 4. (a) Curie temperature $T_C(d)$ of nickel nanowire arrays vs wire diameter d. (b) The log-log plot showing the reduced temperature $[T_C(\infty)-T_C(d)]/T_C(\infty)$ normalized to the Curie temperature for bulk Ni $[T_C(\infty)=631\,\mathrm{K}]$ vs wire diameter. The solid line in (b) corresponds to $\lambda=0.94$ and $\xi_0=22\,\text{Å}$.

ture will be constrained by the wire diameter d, resulting in a reduced Curie temperature defined by

$$T_C(d)=T_C(\infty)\left[1-\left(\frac{\xi_0}{d}\right)^{\lambda}\right] \tag{2}$$

or

$$\frac{T_C(\infty)-T_C(d)}{T_C(\infty)}=\left(\frac{\xi_0}{d}\right)^{\lambda}, \tag{3}$$

where $T_C(d)$ is the Curie temperature for nanowires with diameter d, and $\lambda=1/\nu$ is the shift exponent.

Due to the relatively large diameters, the nanowires are expected to behave as a constrained 3D system [Eq. (3)],[26] without the complexity of 3D to 1D crossover.[29] Figure 4(b) shows a log-log plot of the reduced temperature $[T_C(\infty)-T_C(d)]/T_C(\infty)$ versus wire diameter d, illustrating that the measured values for $T_C(d)$ follow the finite-size scaling relation of [Eq. (3)]. From this figure we obtain $\lambda=0.94$ and an extrapolated value of $\xi_0=22\,\text{Å}$. The observed exponent of $\lambda=0.94$ is lower than the theoretical values predicted by the 3D Heisenberg model ($\lambda=1.4$) and the 3D Ising model ($\lambda=1.58$),[27,28] however both models assume nearest neighbor interactions whereas nickel is a ferromagnet that exhibits longer range interactions. Spin-wave studies of Ni indicate that the magnetic interactions extend beyond the fourth neighbors.[30] For the same reason the critical exponent β for the magnetization of Ni is 0.4, much larger than 0.36 for a 3D Heisenberg system with nearest-neighbor interactions.[31]

It may be noted that Eq. (1), from which Eq. (3) is derived, is valid for T close to $T_C(\infty)$, i.e., in the critical region where $T_C(d)$ is close to $T_C(\infty)$ for systems with relatively large d. Thus for the relatively large diameters of the nickel nanowires, as required by the scaling law, the extrapolated correlation length ξ_0 carries a larger uncertainty. However, the extrapolated correlation length $\xi_0=22\,\text{Å}$ is close to the value of 20 Å reported for polycrystalline nickel thin films,[6] although it is somewhat larger than the values of 4–10 Å obtained for epitaxial single-crystal nickel films.[4,5]

Finally, we comment on the possible effects on T_C due to strain. Large strains are known to exist in thin films, however, the effects on T_C from mismatch in lattice and thermal expansion are rarely incorporated. This is because of the difficulty in quantifying strain and the lack of simple relation between strain and the resultant T_C. In thin films, the problem is further compounded by the variation of strain with film thickness. As a result, practically all finite-size scaling studies in thin films, including all the results mentioned above, neglect any effects due to strain. In the nanowire geometry, as long as the volume fraction of nickel is constant and sufficiently small that all of the strain occurs in the nanowires, the lateral strain is expected to be independent of wire diameter. Thus, an upper limit for such an effect is 4 K, corresponding to the shift in T_C for the largest wire diameter of 500 nm. However, as can be seen from Figure 4(b), since all the data, including that of $d=500\,\text{nm}$, follow the finite-size scaling relation, the actual contribution due to strain is likely to be negligible.

In summary, we have measured the reduction of Curie temperature of Ni nanowires as a function of the nanowire diameter from 30 nm to 500 nm. The mica templates in which nickel nanowires are imbedded enable such measurements for nanowires. The T_C reduction follows a finite-size scaling relationship.

This work was supported by NSF Grant No. DMR-96-32526.

[1] Y. Li and K. Baberschke, Phys. Rev. Lett. **68**, 1208 (1992).
[2] C. A. Ballentine, R. L. Fink, J. Araya-Pochet, and J. L. Erskine, Phys. Rev. B **41**, 2631 (1990).
[3] J. R. Childress, C. L. Chien, and A. F. Jankowski, Phys. Rev. B **45**, 2855 (1992).
[4] R. Bergholz and V. Gradmann, J. Magn. Magn. Mater. **45**, 389 (1984).
[5] F. Huang, G. J. Mankey, M. T. Kief, and R. F. Willis, J. Appl. Phys. **73**, 6760 (1993).
[6] H. Lutz, J. D. Gunton, H. J. K. Schurmann, J. E. Crow, and T. Mihalisin, Solid State Commun. **14**, 1075 (1974).
[7] N. C. Koon, B. T. Jonker, F. A. Volkening, J. J. Krebs, and G. A. Prinz, Phys. Rev. Lett. **59**, 2463 (1987).
[8] H. J. Elmers, J. Hauschild, H. Hoche, U. Gradmann, H. Bethge, D. Heuer, and U. Kohler, Phys. Rev. Lett. **73**, 898 (1994).
[9] C. M. Schneider, P. Bressler, P. Schuster, J. Kirschner, J. J. de Miguel, and R. Miranda, Phys. Rev. Lett. **64**, 1059 (1990).
[10] M. Farle and K. Baberschke, Phys. Rev. Lett. **58**, 511 (1987).
[11] M. Farle, K. Baberschke, U. Stetter, A. Aspelmeier, and F. Gerhardter, Phys. Rev. B **47**, 11 571 (1993).
[12] E. D. Tober, F. J. Palomares, R. X. Ynzunza, R. Denecke, J. Morais, Z. Wang, G. Bino, J. Liesegang, Z. Hussain, and C. S.

Fadley, Phys. Rev. Lett. **81**, 2360 (1998).
[13] G. G. Kenning, J. M. Slaughter, and J. A. Cown, Phys. Rev. Lett. **59**, 2596 (1987).
[14] A. Gavrin, J. R. Childress, C. L. Chien, B. Martinez, and M. B. Salamon, Phys. Rev. Lett. **64**, 2438 (1990).
[15] T. Ambrose and C. L. Chien, Phys. Rev. Lett. **76**, 1743 (1995).
[16] T. Ambrose and C. L. Chien, J. Appl. Phys. **79**, 5920 (1996).
[17] E. E. Fullerton, K. T. Riggs, C. H. Sowers, S. D. Bader, and A. Berger, Phys. Rev. Lett. **75**, 330 (1995).
[18] A. Aharoni, *Introduction to the Theory of Ferromagnetism* (Oxford University Press, New York, 1996).
[19] W. D. Williams and N. Giordano, Rev. Sci. Instrum. **55**, 410 (1984).
[20] J. T. Madsen and N. Giordano, Phys. Rev. B **31**, 6395 (1985).
[21] C. R. Martin, Science **266**, 1961 (1994).
[22] T. M. Whitney, J. S. Jiang, P. C. Searson, and C. L. Chien, Science **261**, 1316 (1993).
[23] J. Meier, B. Doudin, and J. Ph. Ansermet, J. Appl. Phys. **79**, 6010 (1996).
[24] R. Ferre, K. Ounadjela, J. M. George, L. Piraux, and S. Dubois, Phys. Rev. B **56**, 14 066 (1997).
[25] L. Sun, P. C. Searson, and C. L. Chien, Appl. Phys. Lett. **74**, 2803 (1999).
[26] L. Sun, C. L. Chien, and P. C. Searson, J. Mater. Sci. **35**, 1079 (2000).
[27] C. M. Schneider, P. Bressler, P. Schuster, J. Kirschner, J. J. de Miguel, and R. Miranda, Phys. Rev. Lett. **64**, 1059 (1990).
[28] See e.g., H. E. Stanley, *Introduction to Phase Transitions and Critical Phenomena* (Oxford University Press, New York, 1971), p. 46.
[29] K. Binder, in *Finite Size Scaling and Numerical Simulation of Statistical Systems*, edited by V. Privman (World Scientific Press, New York, 1990), p. 174.
[30] S. N. Kaul, Phys. Rev. B **27**, 5761 (1983).
[31] M. Seeger, S. N. Kaul, H. Kronmuller, and R. Reisser, Phys. Rev. B **51**, 12 585 (1995).